Contemporary Mathematics
https://ojs.wiserpub.com/index.php/CM/

Research Article

Real-Time Energy Management Control of Hybrid Electric Vehicles with Dedicated Hybrid Transmission Based on Equivalent Consumption Minimization Strategy and Dynamic Programming

Wang Wei[1], Tian Yi[1], Cai Zhenjiang[2*], Wang Jian[1], Zhang Xiaoyuan[1], Liu Shaofei[3]

[1] School of Statistics and Data Science, HeBei Finance University, Baoding, 071001, China
[2] College of Mechanical and Electrical Engineering, HeBei Agricultural University, Baoding, China
[3] Engineering Research Institute, FOTON Motor Corporation, Beijing, 102206, China
E-mail: czj65@163.com

Received: 9 May 2025; **Revised:** 8 July 2025; **Accepted:** 29 July 2025

Abstract: This paper proposes a real-time energy management strategy for Dedicated Hybrid Transmission (DHT) Hybrid Electric Vehicles based on Equivalent Consumption Minimization Strategy-Dynamic Programming (ECMS-DP), which supports four operating modes: pure electric, boost electric, series and parallel modes. The strategy uses Dynamic Programming (DP) algorithm to solve the Worldwide Harmonized Light Vehicles Test Cycle (WLTC) cycle off-line to obtain the optimal shift line with the objective of energy loss minimization. And the real-time control strategy is based on Adaptive Equivalent Consumption Minimization Strategy (A-ECMS) and the optimal shift line, with minimizing energy loss, engine start/stop times, engine power change and engine speed change as mixed target functions. Then a real-time energy management control system based on ECMS-DP is established. The system utilizes series and parallel Hamiltonian functions to judge the series and parallel modes, and significantly reduces the calibration workload. Through verification in real-vehicle revolving drum test, it has been verified that this strategy can effectively utilize the power battery capacity while maintaining electric balance compared to rule-based strategies such as Rule-Based Threshold Control, and it achieves better fuel economy, with a fuel-saving rate of approximately 5.18%.

Keywords: Hybrid Electric Vehicle (HEV), real-time control, ECMS, energy management, Dedicated Hybrid Transmission (DHT), Dynamic Programming (DP)

MSC: 93C20, 90C39

Abbreviation

DHT	Dedicated Hybrid Transmission
DEM	Drive Electrical Motor
GEM	Generator Electrical Motor
DHE	Dedicated Hybrid Engine
ASS	Active Safety System
DP	Dynamic Programming

DOI: https://doi.org/10.37256/cm.6520257208

ECMS	Equivalent Consumption Minimization Strategy
SOC	State Of Charge
WLTC	Worldwide Harmonized Light Vehicles Test Cycle
NVH	Noise; Vibration; Hardness (problems)
HVB	High-Voltage power Battery

Variables

$u_n(t)$	System input power (kW)
$y_n(t)$	System output power (kW)
v_i	System output power (kW)
$\dot{m}_f(t)$	Fuel massflow (g/s)
$\lambda(t)$	Lagrange factor (-)
c_i	State of Clutch i (1-Closed; 0-Open)
q_{LHV}	Low Heat Value (kJ/kg)
$T_n(t)$	Torque (Nm)
T_{clnt}	The coolant temperature (°C)
i	Gear ratio (-)
ω	Angular velocity (rad/s)
n	Speed (rpm)
η	Efficiency (-)
x	State variable (-)
P	Power (kW)
R_i	Internal resistance (Ω)
V	Voltage (V)
NVH	Ride comfort of vehicle (db)
d	Drive electrical motor
g	Generator electrical motor
e	Dedicated hybrid engine
br	Brake system
h	High voltage power battery
m	Motor
ech	Electrochemical
req	Requirement
$clnt$	Coolant
f	Fuel
wh	Wheel level
act	Action value
p	Parallel
s	Series
chg	Charge
dis	Discharge
oc	Open circle
$strt$	Start

1. Introduction

Major automotive companies worldwide are seeking innovative powertrain system solutions to reduce vehicle emissions and minimize pollution. One of the most effective solutions is the powertrain system that uses a Dedicated Hybrid Transmission (DHT) and a Dedicated Hybrid Engine (DHE). The DHT often integrates multiple electric motors, with current popular configurations incorporating either P2 motors or the combination with P1 and P3 motors. The various combinations of motors within DHT systems create diverse powertrain topologies, enhancing the flexibility in energy management strategy control. The Equivalent Consumption Minimization Strategy (ECMS) achieves a good balance between reducing computational complexity and improving fuel economy, and is thus commonly used for real-time energy management control [1–3]. Another classic approach is the Dynamic Programming (DP)-based offline search for a global optimal energy management strategy, which is often applied in map-based real-time control and serves as a benchmark for comparison with other energy management strategies [4–7].

This study analyzes the structure of a P1 + P3 two-gear, dual-clutch DHT hybrid powertrain system. By applying the DP algorithm with energy loss as the objective function, the optimal solution is obtained through offline simulation of the WLTC cycle, from which the shift strategy is extracted. Additionally, an Adaptive Equivalent Consumption Minimization Strategy (A-ECMS) is employed, where the mixed objective function includes minimizing energy loss, engine start/up number, engine power variation, and engine speed variation. Based on these, a real-time energy management system using ECMS-DP is established, and simulations and real-vehicle tests are conducted to verify the effectiveness of the proposed strategy. The remainder of this paper is organised as follows:

Section 1: Divide the entire DHT HEV powertrain system into several subsystems and establish modular models. The purpose is to achieve modularization of control strategies for distributed development.

Section 2: Focusing on the optimal control problem of DHT HEV energy management. Using DP offline to obtain the optimal control decisions and the optimal trajectory; Deriving the instantaneous optimal energy management strategy (A-ECMS) based on PMP.

Section 3: Propose Real-Time Energy Management Control based on ECMS-DP. This real-time control mainly includes two parts, one is optimal shift control, and the other is optimal operation mode selection and optimal torque distribution. The shift line map is the core of shift control, which is mainly extracted from the optimal solution obtained based on DP; The mode selection and torque distribution are based on PMP.

The main contributions of this study include: firstly, proposing an optimal shift control based on DP, which differs from traditional shift lines based on accelerator pedal position and vehicle speed. This shift line is mainly based on DHE speed and torque; Secondly, the optimal mode selection series and parallel methods has been proposed, which utilizes series and parallel Hamiltonian functions to decide the series and parallel modes.

2. DHT hybrid powertrain system model

This study focuses on the DHT hybrid powertrain system with a P1 + P3 structure. The schematic diagram is shown in Figure 1. The DHT adopts a two-gear, dual-clutch architecture that integrates a generator (P1) and a drive motor (P3). The P1 is directly connected to the engine output shaft, which is linked to the drive shaft wheel through the first and second gear clutches. The P3 is directly connected to the drive shaft wheel.

The vehicle structure shown in Figure 1 is represented by the power flow diagram in Figure 2. One end of the P3 motor (DEM) is connected to the drive shaft, while the other end is connected to the engine via clutches c_1 and c_2. The DHE is connected to the drive shaft through clutches c_1 and c_2. The P1 motor (GEM) is connected to the engine (DHE) through clutch c_2. The High-Voltage power Battery (HVB) is connected to both the DEM and GEM.

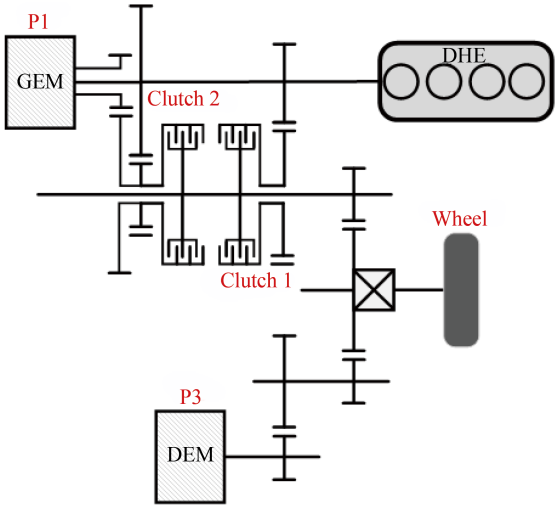

Figure 1. The structure of P1 + P3 hybrid vehicle powertrain

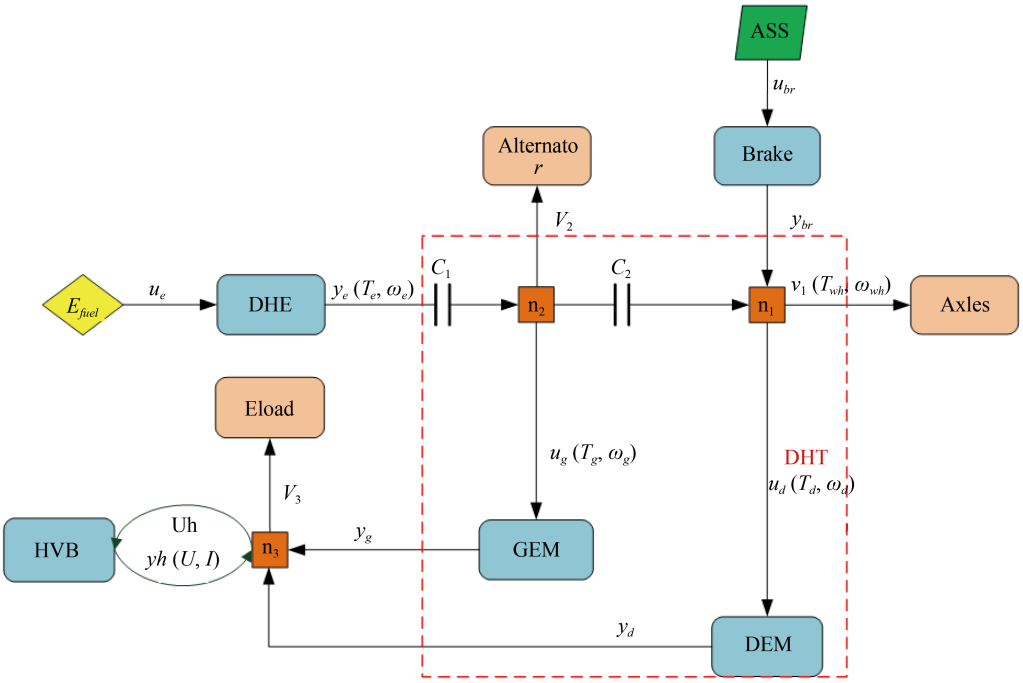

Figure 2. Power flow diagram of power domain system (arrow direction is positive). c_1 and c_2 represent the clutch states; v_1 is the output power at node n_1; v_2 is the input power at node n_2, for example, the input of the alternator (AC generator); the electrical load (Eload) represents the input power v_3 at node n_3

This powertrain domain system supports the following four operating modes (as shown in Table 1):

Mode 1: Pure electric mode driven solely by the DEM.

Mode 2: Boost electric mode is driven by the GEM and DEM motors with the clutch closed.

Mode 3: Clutch c_1 is open, clutch c_2 is closed. The DEM drives directly, while the ENG drives the GEM in series generation mode. This is the series mode.

Mode 4: Clutch closed, both the motor and the engine are engaged for parallel drive mode.

From the torque constraints in Modes 1 and 2 in Table 1, it can be observed that when the engine output torque is zero, meaning the engine is not operating, the system operates in pure electric mode.

Table 1. The operate mode of multi-modal HEV

Mode	c_1	c_2	Torque constraints	Mode definition
1	0	0	$v_1(t) = y_{br}(t) - u_d(t)$, $y_e(t) = 0$, $u_g(t) = 0$ $v_2(t) = -u_g(t)$, $y_e(kt) = 0$	Pure electric mode
2	1	0	$v_1(t) + v_2(t) = y_{br}(t) - u_d(t) - u_g(t)$, $y_e(t) = 0$	Boost electric mode
3	0	1	$v_1(t) = y_{br}(t) - u_d(t)$, $v_2(t) = y_e(t) - u_g(t)$	Series mode
4	1	1	$v_1(t) + v_2(t) = y_{br}(t) + y_e(kt) - u_d(t) - u_g(t)$, $y_e(t) > 0$	Parallel mode

2.1 *Power flow analysis*

Each subsystem in Figure 2 is defined by its input $u_n(t)$ and output $y_n(t)$ [8–12], where $n \in N = \{e, d, g, h, br\}$. The power balance equations at nodes n_1, n_2, and n_3, can be expressed as:

$$\begin{cases} v_1 + u_d - y_{br} - c_1 (c_2 y_e - v_2 - u_g(t)) = 0 \\ v_2 + u_g - c_2 y_e + c_1 (v_1 - y_{br} + u_d) = 0 \\ v_3 - y_d - y_h - y_g(t) = 0 \end{cases} \tag{1}$$

The power balance Equation (1) can be rewritten in the following general form:

$$\Phi(t) v(t) + \sum_{n \in N} (Q_n(t) u_n(t) - F_n(t) y_n(t)) = 0 \tag{2}$$

where $N = \{e, d, g, h, br\}$, the output power $v(t) = \begin{bmatrix} v_1(t) & v_2(t) & v_3(t) \end{bmatrix}^T$, and the connection matrixes are:

$$\Phi(t) = \begin{bmatrix} 1 & c_1(t) & 0 \\ c_1(t) & 1 & 0 \\ 0 & 0 & 1 \end{bmatrix} \tag{3}$$

$$Q_e = \begin{bmatrix} 0 \\ 0 \\ 0 \end{bmatrix}, \; F_e = \begin{bmatrix} c_1(t) c_2(t) \\ c_2(t) \\ 0 \end{bmatrix} \tag{4}$$

$$Q_d = \begin{bmatrix} 1 \\ c_1(t) \\ 0 \end{bmatrix}, \; F_d = \begin{bmatrix} 0 \\ 0 \\ 1 \end{bmatrix} \tag{5}$$

$$Q_g = \begin{bmatrix} c_1(t) \\ 1 \\ 0 \end{bmatrix}, \; F_g = \begin{bmatrix} 0 \\ 0 \\ 1 \end{bmatrix} \tag{6}$$

$$Q_h = \begin{bmatrix} 0 \\ 0 \\ 0 \end{bmatrix}, \; F_h = \begin{bmatrix} 0 \\ 0 \\ 1 \end{bmatrix} \tag{7}$$

$$Q_{br} = \begin{bmatrix} 0 \\ 0 \\ 0 \end{bmatrix}, \; F_{br} = \begin{bmatrix} 1 \\ c_1(t) \\ 0 \end{bmatrix} \tag{8}$$

For different powertrain topologies, the power balance Equation (2) is general. For each architecture, only the connection matrix $\Phi(t)$, $Q_n(t)$, and $F_n(t)$ need to be modified to match the specific powertrain architecture, thereby reducing development costs.

2.2 *Subsystem model*

Each subsystem is modeled using a quadratic relationship between $u_n(t)$ and $y_n(t)$, that is:

$$q_n(t)u_n^2(t) + f_n(t)u_n(t) + e_n(t) + y_n(t) = 0 \tag{9}$$

where:

$$\underline{u}_n(t) \leq u_n(t) \leq \overline{u}_n(t) \tag{10}$$

For the energy storage subsystem, the state equation is as follows:

$$\dot{x}_n(t) = A_n(t)x_n(t) + B_n(t)u_n(t) \tag{11}$$

where:

$$\underline{x}_n(t) \leq x_n(t) \leq \overline{x}_n(t) \tag{12}$$

2.2.1 *The engine*

The input and output power are defined as follows:

$$u_e(t) = q_{LHV}\dot{m}_f(t),\ y_e(t) = T_e(t)\omega_e(t) \tag{13}$$

where $\dot{m}_f(t)$ can be calculated from the engine-specific fuel consumption map.

Based on Equation (9), the simple input-output power relationship of the engine is as follows:

$$f_e(\omega_e(t))\,u_e(t) + e_e(\omega_e(t)) + y_e(t) = 0 \tag{14}$$

where $f_e(\omega_e(t)) = -\dfrac{1}{\eta_e(\omega_e(t))\,q_{LHV}}$; $e_e(\omega_e(t))$ is the error between the engine input and output, and η_e is the engine efficiency.

2.2.2 *The motor*

The input and output power are defined as follows:

$$\begin{cases} u_g(t) = T_g(t)\omega_g(t) = \dfrac{T_g n_g}{9,550},\ y_g = \eta_g u_g \\ u_d(t) = T_d(t)\omega_d(t) = \dfrac{T_d n_d}{9,550},\ y_d = \eta_d u_d \end{cases} \tag{15}$$

where η_g and η_d are the efficiencies of the motors.

Based on Equation (5), the simple input-output power relationship of the motor is as follows:

$$f_m u_m(t) + y_m(t) = 0 \tag{16}$$

where $f_m = -\eta_m$.

2.2.3 *High-voltage power battery*

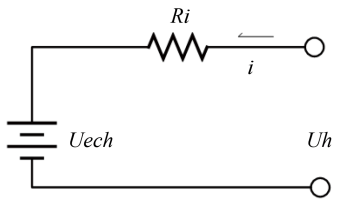

Figure 3. First order battery circuit model

The model of the high-voltage power battery subsystem is a first-order equivalent circuit model designed for control, as shown in Figure 3. Its mathematical model is as follows:

$$q_h u_h^2(t) + f_h u_h(t) + y_h(t) = 0 \tag{17}$$

where $q_h = \dfrac{R_h}{U_{oc}^2}$, $f_h = -1$ is substituted into (17):

$$i_h^2 R_i - u_h(t) + y_h(t) = 0 \tag{18}$$

For the battery, the state equation is expressed as follows:

$$\dot{x}_h(t) = \eta_h \left(y_d(t) + y_g(t) - v_2\right) \tag{19}$$

where η_h is the charging and discharging efficiency.

Let $u_{ech} = \eta_h \left(y_d(t) + y_s(t) - v_2\right) = U_h - iR_i$, where u_{ech} is the electrochemical power. Then, Equation (19) can be rewritten as:

$$\dot{x}_h(t) = u_{ech} \tag{20}$$

The consumption power of the battery is $i^2 R_i$ (Equation (18)), which can also be obtained through the battery cell calculation. The formula is as follows:

$$u_h - u_{ech} = U i - V_{oc} i \tag{21}$$

where:

$$\begin{aligned} V_{oc} &= N_S V_{oc,\ cell} \\ R_i &= \frac{N_S}{N_P} R_{i,\ cell} \end{aligned} \tag{22}$$

where $R_{i,\ cell}$ is the cell internal resistance, N_S is the number of series-connected cells per module, N_P is the number of series-connected cells per module, and V_{oc} is open-circuit voltage obtained from the *SOC* vs OCV characteristic curve.

Equations (18) and (21) should be cross-validated to obtain the most accurate estimate.

2.2.4 *Brake system*

The Active Safety System (ASS) is the output power of the intelligent driving vehicle's braking system. Excluding the braking energy recovery part, the non-recoverable power y_{br} will dissipate in the form of heat. Therefore, the relationship between the input and output power is not considered.

3. Energy consumption model

3.1 *Optimization control problem*

3.1.1 *Objective function*

The goal of HEV energy management is to minimize the cumulative fuel consumption, which is equivalent to minimizing the cumulative energy loss in all subsystems of the vehicle:

$$J = \int_{t_0}^{t_f} \sum_{n \in N} (u_n(t) - y_n(t))\, dt \tag{23}$$

Where $u_n(t) - y_n(t)$ represents the energy loss of the subsystem. Excluding the brake subsystem, the above Equation (23) holds only for $N = \{e,\ d,\ g,\ h\}$.

3.1.2 *State equation*

The state equation is given by Equation (20), where the State Of Charge (SOC) of the battery is $SOC = \frac{x}{Q_c}$, and Q_c is the battery capacity.

3.1.3 *Constraints*

1. Speed constraints for the motor and engine:

$$\begin{cases} \omega_{m\_\min} \le \omega_m \le \omega_{m\_\max} \\ 0 \le \omega_e \le \omega_{e\_\max} \end{cases} \tag{24}$$

2. Torque constraints：

$$\begin{cases} T_{m\_min} \le T_m \le T_{m\_max} \\ T_{e\_min} \le T_e \le T_{e\_max} \end{cases} \tag{25}$$

3. SOC constraints:

$$\begin{cases} SOC_{\min} \le SOC(x) \le SOC_{\max} \\ SOC(N) - SOC(0) = \Delta SOC \end{cases} \tag{26}$$

4. Battery charging and discharging power constraints:

$$\begin{cases} P_{chg\_min} \le P_{chg} \le P_{chg\_max} \\ P_{dis\_min} \le P_{dis} \le P_{dis\_max} \end{cases} \tag{27}$$

5. Engine NVH constraints:

$$NVH_{\min} < NVH < NVH_{\max} \tag{28}$$

3.2 *Energy management based on DP*

The DP algorithm is based on Bellman's optimality theory and adopts a multi-stage decision-making process to find the optimal solution trajectory (red trajectory) in the entire state space grid, as shown in Figure 4, the entire state space grid is discretized horizontally (in the time direction) and vertically (in terms of *SOC*).

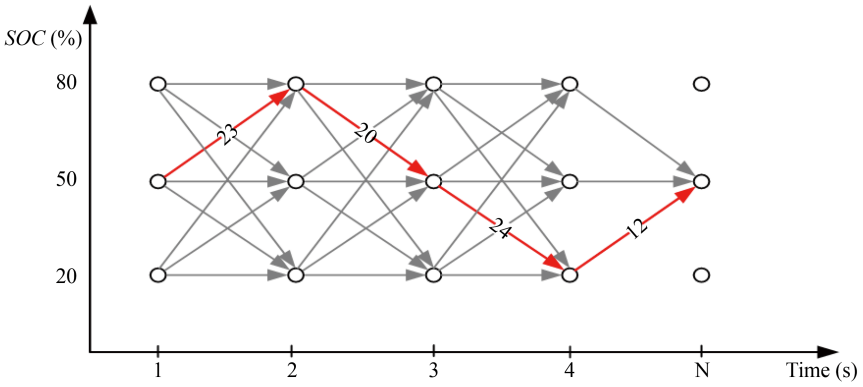

Figure 4. DP discrete grid

In the WLTC driving cycle, use the DP algorithm to solve the optimal control decision $u^* = \left[T_e^*,\ T_g^*,\ T_d^*,\ mode^*,\ \omega_e^*\right]$ for both unloaded and fully loaded vehicle conditions [13, 14]. The process is as follows:

(1) Discretize the *SOC* with a step size of 0.25 and set the sampling time to 1s, as shown in Figure 4.

(2) Based on the longitudinal dynamics model, solve for the wheel-level required torque vector T_{req_wh} and wheel speed vector ω_{wh} during the WLTC cycle.

(3) Determine the constraint conditions (Equations (24)-(27)), including the maximum and minimum speed vectors $\omega_{n\_\min}$ and, $\omega_{n\_\max}$, as well as the maximum and minimum torque vectors $T_{n\_\min}$ and $T_{n\_\max}$ of the whole WLTC cycle, where $n \in N = \{e,\ g,\ d\}$, which can be obtained from the universal characteristics of the motor and engine.

(4) Establish the energy consumption model and power distribution strategy.

(5) Starting from the endpoint of the driving cycle, traverse all feasible grid points in the discrete space and calculate the energy consumption cost, storing the optimal state trajectory.

(6) Select the trajectory with the minimum energy consumption and store the optimal decision u_{ki}^*.

Figure 5 is the Frame of DP-based energy management algorithm, which is divided into three parts: the input module, the output module, and the energy management module. The input module mainly samples the entire WLTC wheel-layer demand torque vector, vehicle speed vector, and discretized constraints (Formulas (24), (25), (26), (27)) at a 1-second interval. The output module is mainly responsible for storing the optimal trajectory matrix, cumulative fuel consumption matrix, etc. The energy management module, as the core module, mainly involves two parts: one is the cost module, and the other is the multi-stage decision-making process based on the Bellman optimality principle.

As shown in Figure 5, the core algorithm of DP-based energy management is the cost model. The difficulty lies in power distribution and optimal gear selection calculation. In the first gear of DHT, the engine cannot be started when the transmission ratio is small and the vehicle speed is low. Therefore, if the vehicle speed is lower than the specific vehicle speed, it cannot enter the parallel mode. Only when the vehicle speed is high, it can enter the parallel mode. According to equation of state (19), the engine power can be expressed as:

$$P_e = T_e \omega_e = P_{wh} - P_b \tag{29}$$

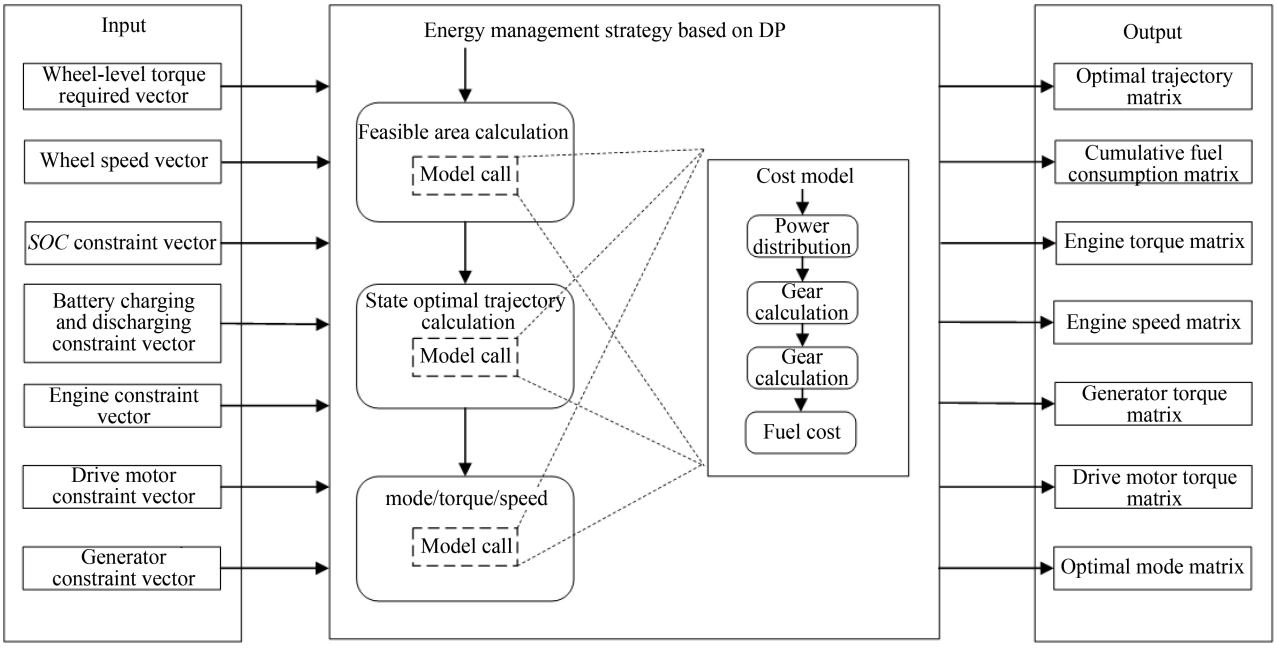

Figure 5. Frame of DP-based energy management algorithm

Based on the power flow diagram shown in Figure 2, the following equation can be obtained:

$$\omega_{wh}(k) = \frac{\omega_e(k)}{i_{DHT}(c)} = \frac{\omega_g(k)}{i_g i_{DHT}(c)} = \frac{\omega_d(k)}{i_d} \tag{30}$$

Where ω_{wh} is the wheel angular velocity, i_{DHT} is the transmission gear ratio, i_d is the ratio from the drive motor to the wheel, i_g is the ratio from the generator to the engine, and c is the clutch corresponding to the gear.

From Equation (30), it can be seen that when the vehicle speed exceeds $\omega_{wh} i_{DHT}(1)$, the engine speed is:

$$\omega_e = \omega_{wh} i_{DHT}(c),\ c \geq 2 \tag{31}$$

For a two-gear DHT, how to obtain the optimal economic gear for the engine while maintaining power performance is an important aspect of HEV energy management. To obtain the distribution of the optimal shift point c^* for the engine, the gear with the minimum system energy loss is selected, that is:

$$i_{DHT}(c^*) = \arg\min \left(\sum_{n \in N} (u_n - y_n) \right),\ c \geq 2 \tag{32}$$

In order to obtain the optimal shift line for low and high load conditions, the optimal shift points for both the unloaded and fully loaded vehicle mass need to be calculated under a given driving cycle.

3.3 *A-ECMS*

3.3.1 *Hybrid objective function*

Based on the principle of minimizing energy loss, as represented by formula (23), the objective function must simultaneously consider both emissions and minimizing the number of engine start/stop. Minimizing emissions primarily involves minimizing changes in engine power, specifically, changes in both series and parallel power. Minimizing the number of engine start/stop refers to determining a reasonable number of engine starts and stops under the premise of minimizing energy loss and emissions. Therefore, the objective function should be transformed into a mixed objective function in vector form as follows:

$$J=\int_{t_0}^{t_f}\left[\sum_{n\in N}\left(u_n(t)-y_n(t)\right)+\varphi_1 u_1\left(T_{clnt},\ \omega_{strt}\right)n_{\text{strt}}+c\varphi_2\mid u_e\left(T_e(t),\ n_{e\_act}(t)\right)\right. \tag{33}$$

$$\left.-u_{e_{\text{act}}}(t)\left|\bar{c}\varphi_2\right|u_e\left(T_{e\_act}(t),\ n_e(t)\right)-u_{e\_act}(t)\mid\right]dt$$

Where u_1 is the fuel energy consumed during each engine start, which is related to the engine coolant temperature T_{clnt} and the target startup speed ω_{strt}. n_{strt} is the accumulated start count vector, and φ_1 and φ_2 are calibratable factors. In the parallel mode, $c=1,\ \bar{c}=0$, in parallel mode, and vice versa.

3.3.2 *Hamiltonian function*

The Pontryagin's Maximum Principle (PMP) is a powerful tool for solving local optimization problems. It allows the redefinition of the optimal control problem under local conditions represented by differential equations and instantaneous minimization. Based on the state Equation (20), the Lagrange multiplier $\lambda(t)$ is introduced, and the Hamiltonian function can be expressed as:

$$\begin{aligned}H=&\sum_{n\in N}\left(u_n(t)-y_n(t)\right)+\varphi_1 u_1\left(T_{clnt},\ \omega_{strt}\right)n_{\text{strt}}+c\varphi_2\mid u_e\left(T_e(t),\ n_{e\_act}(t)\right)\\&-u_{e\_act}(t)\left|+\bar{c}\varphi_2\right|u_e\left(T_{e\_act}(t),\ n_e(t)\right)-u_{e\_act}(t)\mid+\lambda(t)u_{ech}\end{aligned} \tag{34}$$

To identify whether the boundary value of the constraint condition is exceeded, an additional penalty function $\gamma(k)$ is introduced, then (34) can be rewritten as:

$$\begin{aligned}H=&\sum_{n\in N}\left(u_n(t)-y_n(t)\right)+\varphi_1 u_1\left(T_{clnt},\ \omega_{strt}\right)n_{\text{strt}}+c\varphi_2\mid u_e\left(T_e(t),\ n_{e\_act}(t)\right)\\&-u_{e\_act}(t)\mid+\bar{c}\varphi_2\left|u_e\left(T_{e\_act}(t),\ n_e(t)\right)-u_{e\_act}(t)\right|+\left(\lambda(t)+\gamma(t)\right)u_{ech}\end{aligned} \tag{35}$$

Where:

$$\gamma(t)=\begin{cases}0 & \text{if boundary not activated}\\ -K & \text{if upper boundary activated}\\ K & \text{if lower boundary activated}\end{cases} \tag{36}$$

In order to satisfy the *SOC* and NVH constraints (26) and (27), penalty functions are introduced:

$$p\left(SOC(t)\right)=1-\left(\frac{SOC(t)-SOC_{xf}(t)}{(SOC_{\max}-SOC_{\min})/2}\right)^{a} \tag{37}$$

$$p\left(NVH(t)\right)=1-\left(\frac{NVH(t)-NVH_{xf}(t)}{(NVH_{\max}-NVH_{\min})/2}\right)^{a} \tag{38}$$

Where $SOC_{xf}(t)$ and $NVH_{xf}(t)$ are the corresponding reference values, and a takes an odd number. The Hamiltonian function can then be written as:

$$H=\sum_{n\in N}\left(u_n(t)-y_n(t)\right)+\varphi_1 u_1\left(T_{clnt},\ \omega_{strt}\right)n_{\text{strt}}+c\varphi_2\mid u_e\left(T_e(t),\ n_{e\_act}(t)\right) \tag{39}$$

$$-u_{e\_act}(t)\mid+\bar{c}\varphi_2\mid u_e\left(T_{e\_act}(t),\ n_e(t)\right)-u_{e\_act}(t)\mid+(\lambda(t)$$

$$+\gamma(t))p(\text{SOC}(t))p(NVH(t))u_{ech}$$

$$S.T.(24),\ (25),\ (26),\ (27),\ (28) \tag{40}$$

In parallel mode, when $c=1$ and $\bar{c}=0$, the Hamiltonian function H is referred to as the parallel Hamiltonian function, denoted as H_p; conversely, when $c=0$ and $\bar{c}=1$, H is referred to as the series Hamiltonian function, denoted as H_s. The optimal control is then

$$T_n^{*}=\arg\min H \tag{41}$$

Where $n\in N=\{e,\ g,\ d\}$

3.3.3 *Equivalent factor adaptation [14, 15]*

The adaptive algorithm uses the classic PI controller, as shown in Equation (42):

$$\lambda=\lambda_0+K_p\left(x_{rf}-x\right)+K_i\int\left(x_{rf}-x\right)dt \tag{42}$$

x_{rf} is the reference state variable. The above equation has three parameters (λ_0, K_p, K_i) that need to be adjusted, where λ_0 is the optimal initial value corresponding to different initial SOCs obtained through offline simulation using the DP algorithm, and linear interpolation is used to determine the value.

4. Real-time energy management control

4.1 *DP-based shift strategy*

The Dynamic Programming (DP) algorithm solves the WLTC cycle offline in a backward manner. The optimal state trajectory for different initial SOCs and the engine operating point distribution for different gears are obtained, as shown in Figures 6 and 7.

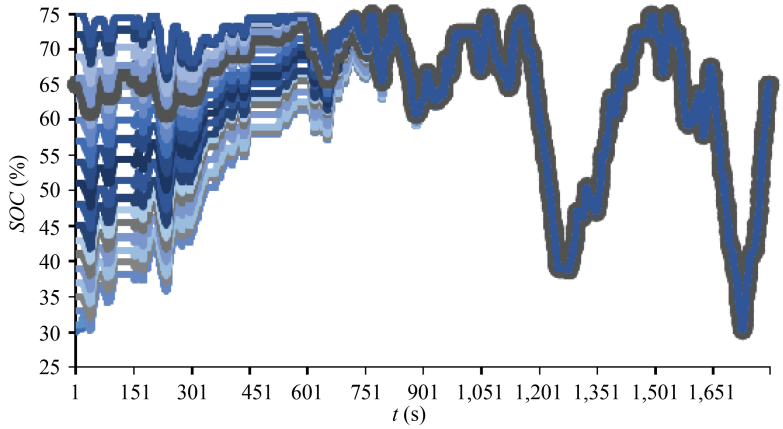

Figure 6. The Optimal *SOC* trajectory of WLTC using DP

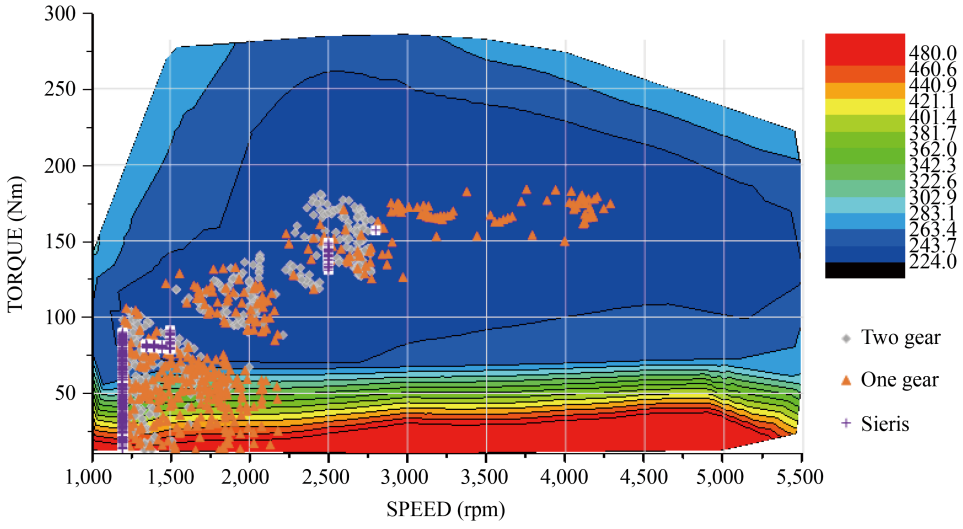

Figure 7. DHE optimal operating point distribution

Considering cost and calibration continuity, domestic OEMs adapt the shift strategy of hybrid vehicles based on traditional vehicles. The shift MAP is based on the Accelerator pedal position (App) and vehicle speed (u_a) [16, 17].

Table 2. Powertrain parameters

Component	Parameter	Value
ENG	Displacement/L	1.5
	Maximum power/Kw	130
	Maximum speed/r·min^{-1}	6,000
	Maximum torque/N·m	283
GEM	Maximum power/Kw	78
	Maximum torque/N·m	95
DEM	Peak power/Kw	135
	Peak torque/N·m	315
DHT	Number of engine gears/-	2
	Number of motor gears/-	/
Hvbat	Battery capacity/Ah	20
	Battery energy/kWh	2
	Rated voltage/V	400
	Maximum current/A	400

In this study, the HEV uses a two-gear, two-clutch DHT with a P1 + P3 architecture. Table 2 lists the parameters of each component. The shift map of this DHT is not related to vehicle velocity (u_a) or Accelerator pedal position (App), as shown in Figure 8. The shift point distribution is chaotic, which is difficult to obtain downshift and upshift lines.

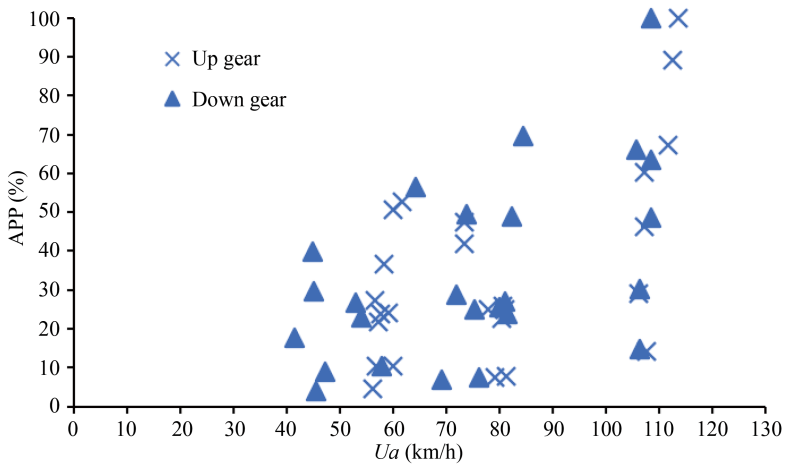

Figure 8. Shift point distribution based on App and vehicle velocity

Unlike traditional vehicles, HEV have multiple power sources. The accelerator pedal position reflects the driver's demand, which must be met by both the motor and engine. Therefore, the engine shift map should be related to engine speed and torque, as shown in Figure 9. The distribution of upshift and downshift points is significantly more concentrated compared to Figure 8, making it easier to obtain the shift lines. As shown in Figure 9, considering drivability, isolated shift points (marked in circles) are not considered in the upshift line.

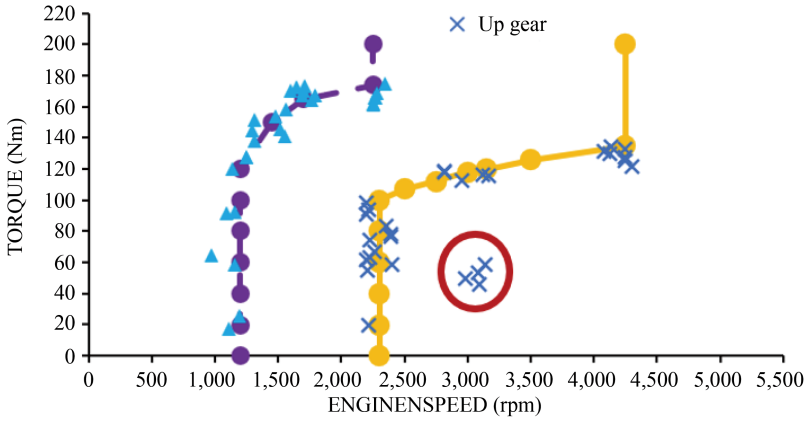

Figure 9. Shift point distribution based on engine torque and engine speed extracted from the optimal solution obtained using DP

Thus, the shift strategy should be based on the DHE speed and DHE torque upshift and downshift MAP.

4.2 *Real-time energy management control based on ECMS-DP*

For the DHT shift strategy in real-time energy management control, DP is used to solve the WLTC cycle offline to obtain the shift line shown in Figure 9, while A-ECMS is used for energy torque distribution, mode determination, and start/stop control.

Figure 10 shows the frame of the real-time energy management, which mainly includes the shift control module based on the DP shift line (Figure 9); the PMP module is established according to the Hamiltonian function (Formula (39)) and based on PMP (Formula (39)), aiming to obtain the optimal decision; the subsystem module is established according to the subsystem models, and the constraint condition module is established according to the constraint conditions; the demand speed and speed calculation module realizes the discretization of engine torque in parallel mode and the discretization of engine speed in series mode. Among them, the demand torque and speed in series mode are mainly based on the optimal power line of the engine.

The real-time energy management control based on ECMS-DP uses a time-sharing call to calculate the series and parallel Hamiltonian functions H_s and H_p, as shown in the following Figure 10. Modular subsystem and PMP modules use 5 ms task, 5 ms for calculating H_p and 5 ms for calculating H_s. In this alternative calculation, such alternate calculation is equivalent to 10 ms for calculating once H_p and H_s, while other modules use 10 ms task.

4.2.1 *Desired mode determination*

The determination of the desired series or parallel mode is mainly based on the series and parallel Hamiltonian functions. If the condition in Equation (43) is satisfied, the system enters the desired parallel mode; otherwise, it enters the non-parallel mode. However, mode switching delays and hysteresis operations must also be considered.

$$\min(H_p) \leq \min(H_s) \tag{43}$$

4.2.2 *Optimal reference SOC*

For a fixed driving path, the calculation of the equivalent factor adaptive reference state variable x_{rf} mainly uses the DP algorithm to offline obtain the optimal *SOC* trajectory, as shown in Figure 6, and the linear interpolation algorithm is used to calculate it.

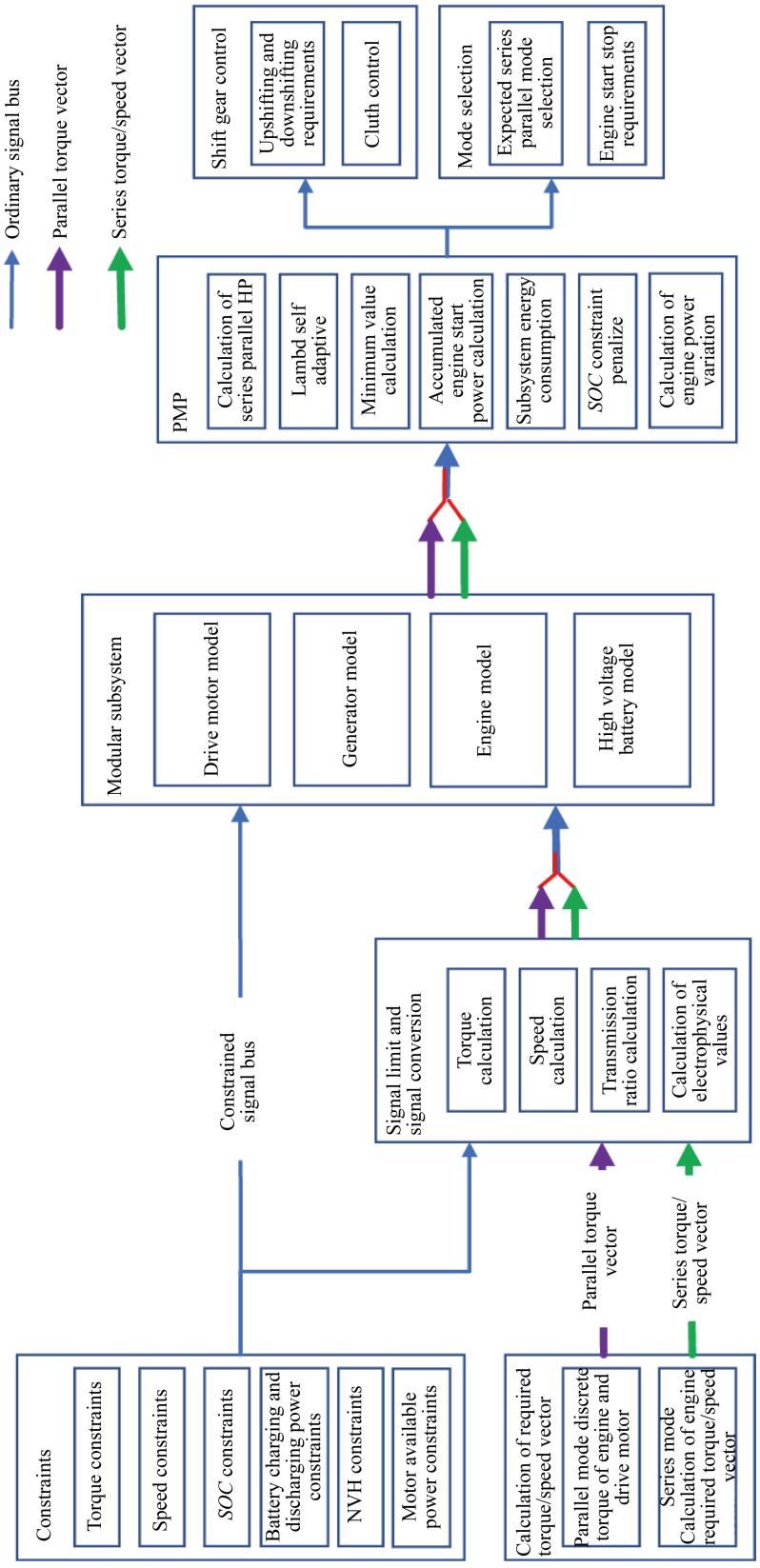

Figure 10. The real-time energy management frame based on ECMS-DP

5. Real vehicle validation

To verify the effectiveness and rationality of the proposed ECMS-DP-based real-time energy management strategy, the strategy was integrated into the Power Domain Control Unit (PDCU) and subjected to a real-vehicle WLTC cycle dynamometer test. The test results were compared with those of the Rule-Based Threshold Control. The Power Domain Control Unit (PDCU) adopts the VCU 8.1 32-bit hardware platform from United Automotive Electronic Systems Co., Ltd. (UAES), and the dynamometer test bench used is the emission dynamometer test bench from AVL.

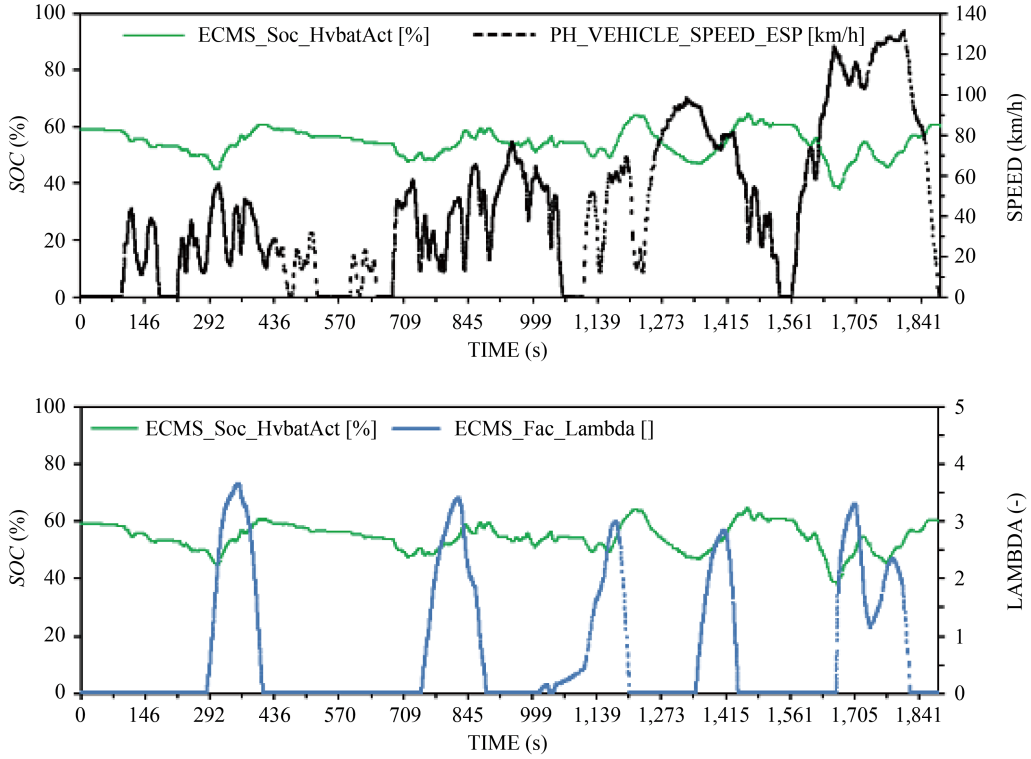

Figure 11. *SOC* vs. λ in WLTC cycle test

In order to effectively verify the fuel economy of the HEV during the WLTC cycle, the test requires that the battery remain in energy balance throughout the cycle, meaning $\Delta SOC = 0$ as per Equation (26). As shown in Figure 11, the initial *SOC* of the entire WLTC cycle is 60%, and the terminal *SOC* is also 60%, indicating that the energy management strategy can maintain electrical balance throughout the WLTC cycle. It can be seen that as the equivalent factor (λ) increases, the cost of generation is higher under the electrical balance constraint, leading the strategy to favor starting the engine to drive. However, under the constraint of $\Delta SOC = 0$, the fluctuation range of *SOC* is about [37%, 70%], which does not make full use of the power battery.

One of the main aspects of the HEV energy management strategy is the selection between series and parallel modes. In this study, the series and parallel Hamiltonian functions are primarily used for this purpose. If the calculation satisfies the condition in Equation (43), the system enters the desired parallel mode; otherwise, it enters the non-parallel mode. To avoid frequent mode switching, delays and hysteresis are considered. As shown in Figure 12, when the minimum value of ECMS_H_HamltFunctionSerlMin (H_s) is greater than that of HamltFunctionParlMin (H_p), the system operates in parallel mode. During the low-speed stage of the WLTC cycle (300 s-400 s), series mode is primarily used, with the engine speed around 1,800 rpm and torque around 110 Nm, located in the engine's efficient zone (Figure 7). During the mid-speed stage (680 s-1,100 s), the minimum values of the series and parallel Hamiltonian functions fluctuate significantly, leading

to frequent gear shifts. As shown in Figure 12, the minimum values of the Hamiltonian function should be filtered. In the high-speed stage (1,500 s-1,880 s), parallel mode is primarily used, and the corresponding equivalent factor is relatively large (Figure 11). Of course, the entire driving process is also related to the driver's driving habits.

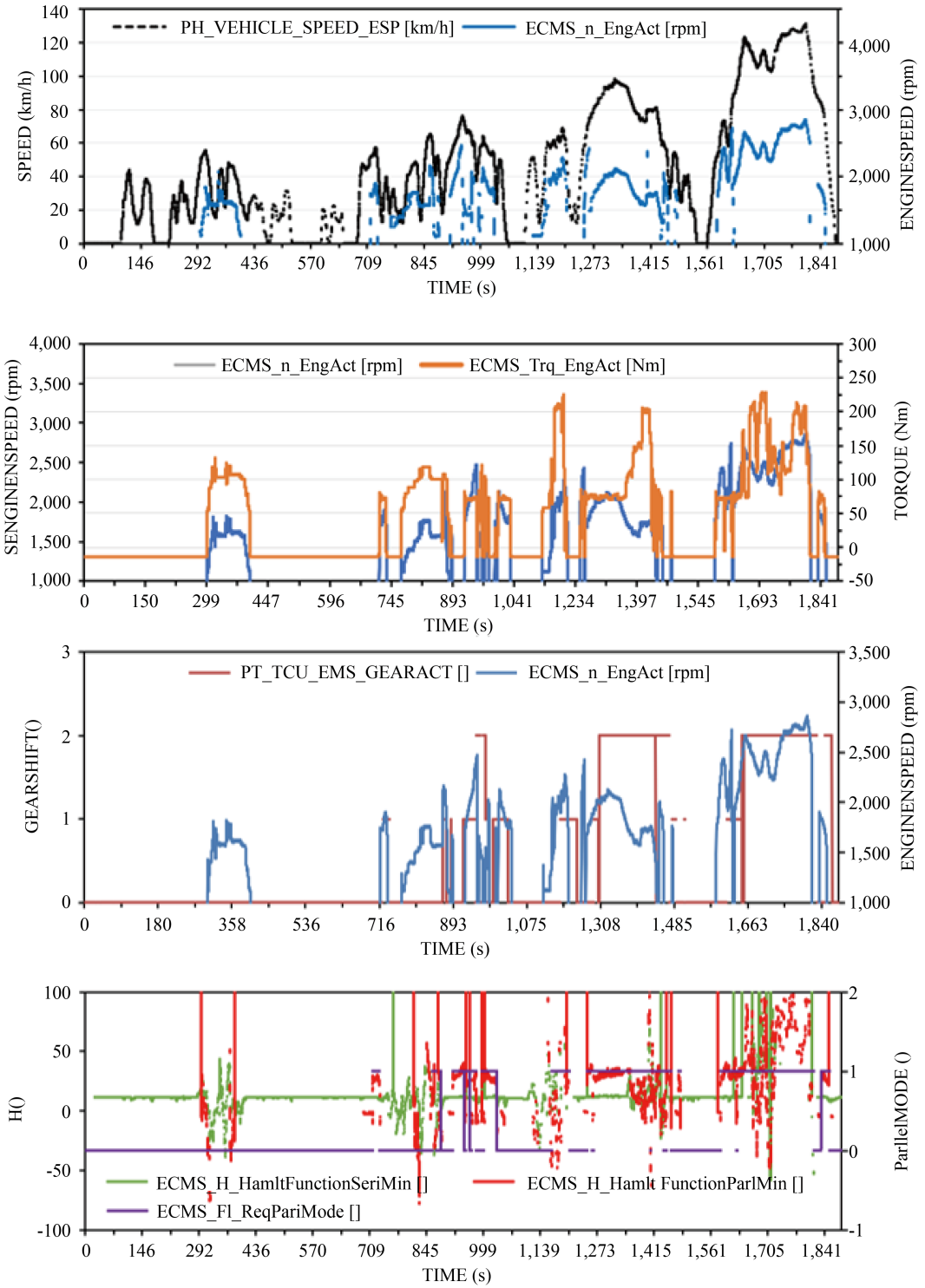

Figure 12. Selection of series-parallel mode in WLTC cycle test

Figure 13 shows the comparison between the ECMS-DP-based strategy and the Rule-Based Threshold Control. The Rule-Based Threshold Control does not maintain electrical balance throughout the entire WLTC cycle, with an initial *SOC* of 63%, and a termination *SOC* of 58%. In contrast, compared with the ECMS-DP-based strategy, the *SOC* fluctuation range is smaller, approximately between [45%, 65%]. When comparing the Rule-Based Threshold Control instantaneous fuel consumption (PT_FUEL_C NSMASSFLOW) and the ECMS-DP-based energy management strategy instantaneous fuel consumption (ECMS_Fuel_EngMassFlow) of the whole cycle, it can be observed that even though the Rule-Based Threshold Control does not maintain electrical balance, the engine operates for a longer period. As a result, the cumulative fuel consumption of the Rule-Based Threshold Control is still higher than that of the ECMS-DP-based strategy. The fuel consumption per 100 kilometers for the Rule-Based Threshold Control is 6.57 L, while for the ECMS-DP-based energy management strategy, it is 6.22 L.

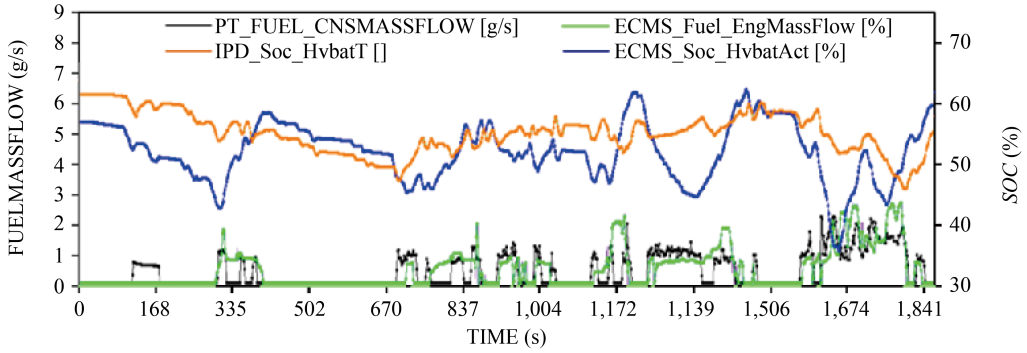

Figure 13. Comparison between ECMS-DP-based and Rule-Based Threshold Control in WLTC cycle test: FUELMASSFLOW vs *SOC*

6. Conclusions

This paper proposes a real-time energy management strategy for DHT HEV based on ECMS-DP, with the goal of minimizing energy loss as the objective function. The aim is to decouple the subsystems to facilitate distributed development. The shift control strategy is derived offline using the DP algorithm and extracting the optimal shift points from the WLTC cycle. The strategy is combined with A-ECMS, using a hybrid objective function and applying the PMP to directly solve the optimal control problem. Compared to the Rule-Based Threshold Control, this approach does not require a large amount of calibration work (such as calibration tables and expert experience). To validate the effectiveness of the proposed strategy, a real vehicle hub test was conducted. The results show that the strategy effectively utilizes the battery capacity while maintaining electrical balance and provides better fuel economy compared to the Rule-Based Threshold Control, with a fuel-saving rate of approximately 5.18%.

Acknowledgement

The authors would like to thank the anonymous reviewers for their valuable comments and suggestions to improve the quality of the paper.

Disclosure

The authors declare no potential conflicts of interest with respect to the research, authorship, and/or publication of this article.

Conflict of interest

The authors declare that they have no known competing financial interests or personal relationships that could have appeared to influence the work reported in this paper.

References

[1] Muthyala P, Mayank M, Bülent N, Han SE, Uzunolu B, Kaydeci AB, et al. Comparative study of real-time A-ECMS and rule-based energy management strategies in long haul heavy-duty PHEVs. *Energy Conversion and Management: X*. 2024; 23: 100679. Available from: https://doi.org/10.1016/j.ecmx.2024.100679.

[2] Delprat S, Jimmy L, Thierry MG, Rimaux J. Control of a parallel hybrid powertrain: optimal control. *IEEE Transactions on Vehicular Technology*. 2004; 53(3): 872-881. Available from: https://doi.org/10.1109/TVT.2004.827161.

[3] Brunelli L, Capancioni A, Cane S, Cecchini G, Perazzo A, Brusa A, et al. A predictive control strategy based on A-ECMS to handle zero-emission zones: performance assessment and testing using an HIL equipped with vehicular connectivity. *Applied Energy*. 2023; 340: 121008 Available from: https://doi.org/10.1016/j.apenergy.2023.121008.

[4] Liu C, Li X, Chen XLK. Real-time energy management strategy for fuel cell/battery vehicle based on speed prediction DP solver model predictive control. *Journal of Energy Storage*. 2023; 73: 1-12. Available from: https://doi.org/10.1016/j.est.2023.109288.

[5] Ma M, Xu E, Zheng W, Qin J, Huang Q. The optimized real-time energy management strategy for fuel-cell hybrid trucks through dynamic programming. *International Journal of Hydrogen Energy*. 2024; 59: 10-21. Available from: https://doi.org/10.1016/j.ijhydene.2024.01.361.

[6] Wang W, Cai Z, Liu S. Design of real-time control based on DP and ECMS for PHEVs. *Mathematical Problems in Engineering*. 2021; 2021(1): 6667614. Available from: https://doi.org/10.1155/2021/6667614.

[7] Yang Y, Pei H, Hu X, Liu Y, Hou C, Cao D. Fuel economy optimization of power split hybrid vehicles: a rapid dynamic programming approach. *Energy*. 2019; 166: 929-938. Available from: https://doi.org/10.1016/j.energy.2018.10.149.

[8] Romijn C, Donker T, Kessels J, Weiland S. Real-time distributed economic model predictive control for complete vehicle energy management. *Energies*. 2017; 10(8): 1096. Available from: https://doi.org/10.3390/en10081096.

[9] Romijn TCJ, Donkers MCF, Kessels JTBA, Weiland S. A distributed optimization approach for complete vehicle energy management. *IEEE Transactions on Control Systems Technology*. 2017; 27(3): 1-17. Available from: https://doi.org/10.1109/TCST.2018.2789464.

[10] Liu Y, Canova M, Wang YY. Distributed energy and thermal management of a 48-V diesel mild hybrid electric vehicle with electrically heated catalyst. *IEEE Transactions on Control Systems Technology*. 2020; 99: 1-14. Available from: https://doi.org/10.1109/TCST.2020.2997868.

[11] Romijn TCJ, Pham TH, Wilkins S. Modular ECMS framework for hybrid vehicles. *IFAC-PapersOnLine*. 2020; 22(5): 128-133. Available from: https://doi.org/10.1016/j.ifacol.2019.09.021.

[12] Wang W, Jian W, Shaofei L, Yi T, Xiaoyuan Z, Tianyu D, et al. Modular ECMS framework for hybrid vehicles energy management. *Modern Electronics Technique*. 2023; 46(17): 179-186. Available from: https://doi.org/10.16652/j.issn.1004-373x.2023.17.034.

[13] Irani F. *On Dynamic Programming Technique Applied to A Parallel Hybrid Electric Vehicle*. Sweden: Chalmers University of Technology; 2009.

[14] Wei W. *The Study on Key Technologies of Real-time Control in Powertrain Domain of Hybrid Electric Pickup Truck*. Hebei: Hebei Agricultural University; 2021.

[15] He H, Shou Y, Song J. An improved A-ECMS energy management for plug-in hybrid electric vehicles considering transient characteristics of engine. *Energy Reports*. 2023; 10: 2006-2016. Available from: https://doi.org/10.1016/j.egyr.2023.08.085.

[16] Lin C, Hou R, Qi Z. A redundant shift control strategy for AMT based on Battery Electric Vehicle. In: *2014 IEEE Conference and Expo Transportation Electrification Asia-Pacific (ITEC Asia-Pacific)*. Beijing, China: IEEE; 2014. Available from: https://doi.org/10.1109/ITEC-AP.2014.6940656.

[17] Li Y, Chang S, Wei Y. Shift strategy of AMT vehicle based on speed and torque control. *China Mechanical Engineering*. 2011; 34(1): 57-64. Available from: https://doi.org/10.1111/j.1365-2761.2010.01212.x.